A SEARCH FOR EFFECTIVE FLAVOUR CHANGING NEUTRAL CURRENTS IN K_L^0 DECAYS.

Yale University:
M. Mannelli, H.B. Greenlee, H. Kasha, E.B. Mannelli, S.F. Schaffner, M.P. Schmidt

Brookhaven National Laboratory:
R.K. Adair, E. Jastrzembski, R.C. Larsen, L.B. Leipuner, W.M. Morse

Presented by: Marcello Mannelli

Abstract

A dedicated search for the decays $K_L^0 \to \mu e$, $K_L^0 \to ee$ and $K_L^0 \to \mu\mu$, was carried out at the Brookhaven National Laboratory AGS (E780). The data obtained were also used in a search for the three-body decays $K_L^0 \to \pi^0 l^+ l^-$. The two body modes were normalized to the kinematically similar, CP violating, decay $K_L^0 \to \pi^+\pi^-$; whereas the three body modes were normalized to the decay $K_L^0 \to \pi^0\pi^+\pi^-$.

The search was performed on a sample of K^0 mesons produced in the forward direction by the interactions of 29 GeV protons on a copper target, and decaying in a 3 meter long region, starting 7.26 meters downstream of the target. The detector consisted of a single magnet spectrometer augmented by a hydrogen Cerenkov counter and a lead glass electromagnetic calorimeter, for electron identification, and by a range stack, for muon identification.

1 Motivation

Despite its phenomenological success, the Standard Model has several shortcomings. For example, no motivation is given for the apparent replication of fermion generations. Furthermore, spontaneous symmetry breaking (SSB) through the standard Higgs sector introduces a host of arbitrary parameters, which severely limit the model's predictive power. The Higgs mechanism of symmetry breaking also fails to provide a natural way of obtaining the gauge hierarchy envisaged in Grand Unified Theories. Finally, although the Standard Model with three generations provides a natural way for introducing CP violation in the Weak sector[1], no explanation for the smallness of strong CP violation is given.

Future machines such as the SSC, and perhaps the LHC or CLIC, should provide us with direct probes of at least some of these questions (SSB in particular), in the meantime however, valuable insight may be gained from the study of some low energy phenomena. In particular, effective flavour changing neutral currents in the Standard Model are highly suppressed, and lepton number violation is forbidden. However, these processes are endemic to most attempts at solving the questions the Standard Model leaves unaddressed.[2][3][4][5][6]

The sensitivity of a particular one from this class of processes, as a probe for new physics, is very model dependent: there exists no single process which best constrains new interactions. On the other hand, for a wide class of models, rare kaon decays do provide the most sensitive testing ground accessible with today's technology.

2 The experimental situation: challenges and strategies.

Note that the rare two-body modes of interest: $K_L^0 \to \mu e$, $K_L^0 \to \mu\mu$, $K_L^0 \to ee$, are kinematically similar not only to each other, but also to the relatively abundant, CP violating, mode $K_L^0 \to \pi^+\pi^-$. Experimentally this is a tremendous bonus, since it allows for reliable measurements of the spectrometer resolution and a relatively straight-forward estimate of the sensitivity. Explicitly, distributions obtained for the $K_L^0 \to \pi^+\pi^-$ sample, (such as reconstructed mass and target angle), can be easily extrapolated (to account for the kinematic differences) to the distributions which one would expect for an ensemble of 'rare' events. Since the corrections required are quite small, there is little room for error. Furthermore, the relative acceptances of the rare modes to the $K_L^0 \to \pi^+\pi^-$ mode can be reliably understood; they are mostly accounted for by differences in the geometric acceptance to muons, which are required to be contained in the range stack, and by a bias in the trigger, induced by the requirement that pions pentrate the lead glass calorimeter array. Efficiencies of the different particle identification requirements can be accurately determined and thus taken into account; other inefficiencies (for example tracking inefficiencies due to both chamber inefficiency at high rates, and reconstruction inefficiency in the presence of accidental hits) will cancel in the ratio. The absolute normalization obtained from the $K_L^0 \to \pi^+\pi^-$ sample can then be used to obtain the sensitivity for the rare modes. The decay $K_L^0 \to \mu\mu$ ($Br = (9.1 \pm 1.9) \times 10^{-9}$)[7], can serve as a (gross) check of the sensitivity, as well as a useful test of the signal isolation techniques.

A fundamental challenge in the search for $K_L^0 \to \mu e$ is provided by the potentially large background from the decay chain:

$K_L^0 \rightarrow \pi e \nu_e$ (K_{e3}) followed by: $\pi \rightarrow \mu \nu_\mu$.

This decay chain results in the 'correct' pair of charged particles in the final state. In the case where the ν_e takes no energy, and the ν_μ is emitted backward with respect to the π original direction, only 8.5 MeV of energy are lost to the ν_μ, in the kaon rest frame. Thus, in the limit where the ν_e from the K_{e3} decay takes little energy in the kaon center of mass frame, this decay chain can indeed closely approximate the signal.

However, the matrix element for K_{e3} decays vanishes for zero neutrino energy. In the relevant region it can be approximated by:

$$P(E_\nu \leq E') \approx 0.04 \times (\tfrac{E'}{50MeV})^3$$

So: $P(E\nu \leq 1MeV) \approx 3 \times 10^{-7}$. Given (approximately) a 1.5% probability for a pion to decay before the magnet we then obtain an effective branching ratio:

$$Br(K_L^0 \rightarrow \pi e \nu \rightarrow' \mu e') \approx 5 \times 10^{-9}$$

with a maximum recontructed mass of 489 MeV/C^2.

An ultimately more pernicious variation on the above is given by those instances in which the π decays close to the magnet mid-plane, thus distorting the momentum measurement. The q-value for the decay $\pi \rightarrow \mu\nu$ is 30 MeV, so that, in the extreme case of the π decaying in the bend plane and at 90^0 to its direction of flight, the laboratory momentum assigned to the μ can differ by as much as $\frac{30}{220} = 13.6\%$ with respect to the original π momentum (the P_t kick of the spectrometer magnet is 220 MeV/c). Whereas the effective branching ratio for such events is smaller than that for the class of events discussed above, these can lead to background events which reconstruct to the K^0 mass. For the class of events which encroach on the K^0 mass, the actual laboratory energy of the μ differs by as much as 30% from the mismeasured momentum, therefore a second measurement of the μ energy, to an accuracy of a few percent, can effectively discriminate against that background. Since the irreducible error in a range measurement of the energy, due to straggling, is about 5%, such a measurement can be accomplished with a range stack. A comparison of the muon range with the momentum measured in the spectrometer will also discriminate strongly against events involving π punch-through.

The spectrometer was designed to achieve a mass resolution no worse than $\sigma \approx 2$ MeV/c^2, and a resolution for the angle of the kaon momentum vector of better than 1 mr. For events in which the decay products of the kaon are bent outward(away from the beam line) by the spectrometer magnet, the mass resolution, in particular, will be irreducibly worse than that for events in which the decay particles are bent inwards. Therefore the experiment was designed to optimize acceptance to inbending events, even at the expense of outbending ones. Since the precision of these measurements is such that they will be vitiated by multiple and single scatters through even a relatively small amount of material, the detector is designed so as to minimize the mass presented to the incident particle flux before the last of the four spectrometer mini-drift chambers.

With the above set of constraints the background to the $K_L^0 \rightarrow \mu e$ mode is estimated, by Monte Carlo methods, to have a branching ratio of a few times 10^{-11}. Thus the experiment should be able to reliably isolate such events at a level of 10^{-10}.

3 General overview of the detector

The neutral beam line was designed to define an angular acceptance of $35\mu sr$ at 0^0 to the incident proton beam, with a vertical to horizontal aspect ratio of 6:1 .

Figure **3.1** shows a schematic view of the E780 detector. The detector configuration is essentially a rather classic one: the spectrometer consists of four mini-drift wire chamber packs (A,B,C,D), arranged in pairs about a single dipole magnet, with a P_t kick of 220 MeV/c; the particle identification is done by an atmospheric pressure H_2 Cerenkov detector, a lead glass array, and finally a muon range stack.

The use of mini-drift chambers obtains good position resolution in the spectrometer ($\approx$ 300 microns at running intensity) which allows for a rather compact layout of the detector, while allowing the necessary kinematic resolution. Indeed, the entire spectrometer measures only 280" in length, from the first to the last chamber, and the larger chambers span but 40" $\times$ 40". Aside from obvious advantages in the cost of the apparatus, the compactness of the detector results in a smaller rate of π decay, which as discussed previously is an important mechanism for generating background. Each chamber pack had X,X',Y and Y' views [Fig.**3.2**]; the B station also included a Θ plane at 14^0 to the vertical (Y), to resolve X-Y ambiguities.

At the cost of exposing the drift chambers to the neutral beam flux, we opted to use a single arm architecture for the spectrometer. This was motivated by consideration of the difficulty in reducing the neutral beam halo sufficiently to benefit from a double arm configuration, without incurring incommensurate losses in the acceptance of either (or both) the neutral beam line and the spectrometer itself.

In order to keep the detector dimensions at a minimun, the Cerenkov counter was placed between the C and D chamber packs. Thus an important design criterion for that detector was that it present a minimum amount of material to the beam. To that end we adopted the excellent design of Carithers *et al.*[8], and indeed went as far as to use large parts of their physical apparatus, with appropriate modifications [Fig.**3.3**]. The essential design feature of the Cerenkov detector lies in its use of 2 sets of reflecting surfaces.

The electromagnetic calorimeter consisted of an array of 16 $\times$ 16 blocks of lead glass, with a hole for the neutral beam of 6 $\times$ 2 blocks; each block measures 2.5" $\times$ 2.5" $\times$ 20". The radiation length of this glass is $\approx$ 1", so that the array presents about 20 radiation lengths to a normally incident particle.

The E, G, H and I counter arrays [Fig.**3.1**] were all involved in the trigger level particle identification. Immediately downstream of them was the muon range stack.

The energy resolution of the range stack needed to be reasonably well matched to the irreducible error due to straggling, which is about 5%. The range stack consisted therefore of 16 layers of steel, of thickness corresponding to a sampling of $\approx 10\% \frac{\Delta E}{E}$, each instrumented with an array of scintillation counters. A muon penetrating to the last counter would have an energy of 9 GeV.

For the purposes of trigger level particle identification, the detector was logically and physically divided into quadrants about the neutral beam. Electrons were required to register a hit in one cell of the Cerenkov counter ($>$ 95% efficient), and to deposit at least 1.2 GeV in the corresponding quadrant of the lead glass. Muons were required to penetrate 42 inches of steel, to the I scintillation counter array, while pions were required to penetrate the lead glass, but to stop short of the H array.

These particle identification triggers were paired from quadrants on the left and on the right of the beam, and placed in coincidence with bend-view information from the drift chambers, to form the fast trigger.

4 Results

Here I describe results obtained from the analysis of data collected in the winter and spring of 1987[9], shortly after significant parts of the detector had to be rebuilt following a catastrophic fire in the fall of 1986. Figures 4.1a,b show mass and θ^2 distributions for a sample of $K^0 \to \pi^+\pi^-$ events (θ is defined as the angle between the line joining the kaon decay vertex to the target, and the reconstructed kaon momentum vector). The mass distribution is consistent with a resolution of $\sigma = 2.1$ MeV/c^2; the θ^2 distribution is such that requiring $\theta^2 \leq 10^{-6}m_K^2$ will exlude few, if any, good two-body events. In the analysis of the rare decay modes, and in particular for the decay $K_L^0 \to \mu e$, $\frac{\mu}{\pi}$ discrimination is crucial and fairly selective cuts were implemented. These included several track continuity criteria, aimed at revealing kinks due to π decay in flight, as well as the requirement that the energy of the muon, as measured in the range stack, be at least 80% of the momentum measured in the spectrometer, and that the energy deposited in the lead glass be consistent with a minimum ionizing track. Since electron identification is not crucial, only loose requirements were made of candidate electrons: they had to have a hit in the appropriate quadrant of the Cerenkov counter (a condition already required by the trigger), and had to deposit at least 75% of their energy in the lead glass calorimeter.

A further cut was made on the momentum asymmetry R of the two tracks involved in an event: $R = (P_1 - P_2)/(P_1 + P_2)$.

For the $K_L^0 \to \mu\mu$ and $K_L^0 \to ee$ samples we required $\mid R \mid \leq 0.5$, whereas for the $K_L^0 \to \mu e$ sample we required $R \leq 0.6$ (here we set $P_1 = P_\mu, P_2 = P_e$); these cuts were better than 95% efficient for good Monte Carlo generated events.

The distributions obtained with those cuts in place are shown in figures 4.2a,b,c. No candidate events are found for $K_L^0 \to \mu e$ and $K_L^0 \to ee$, whereas two events are found, consistent with $K_L^0 \to \mu\mu$.

Next we estimate the sensitivity of our measurement; the basic strategy is to use the sample of $K^0 \to \pi^+\pi^-$ decays, to obtain the absolute normalization, and to reconstruct the K_L^0 spectrum in our beam. The K_L^0 spectrum is used as input to calculate the acceptance of the rare modes, relative to that for $K_L^0 \to \pi\pi$. The sensitivity for the rare modes is then simpy given by the product of the absolute normalization times the relative acceptance for the mode in question.

The results are summarized in Table 1, where we explicitly separate the sample into in-bending and out-bending events. We observe no events consistent with either $K_L^0 \to \mu e$ or $K_L^0 \to ee$; this enables us to place 90% confidence limits on those decay modes of:

$Br(K_L^0 \to \mu e) \leq 6.7 \times 10^{-9}$ and $Br(K_L^0 \to ee) \leq 4.5 \times 10^{-9}$.

Furthermore we observe two events consistent with the decay $K_L^0 \to \mu\mu$, in agreement with expectation.

In-bending		Out-bending		
$\sigma\ M_K(\pi^+\pi^-)$	2.1 MeV/c^2	$\sigma\ M_K(\pi^+\pi^-)$	3.8 MeV/c^2	
$N(K^0 \to \pi^+\pi^-)$	3350	$N(K^0 \to \pi^+\pi^-)$	1103	
$\pi^+\pi^-$ Prescale	128	$\pi^+\pi^-$ Prescale	128	
K_L^0 fraction	76%	K_L^0 fraction	35%	
Differential acceptance $(K_L^0 \to l^+l^-/K_L^0 \to \pi^+\pi^-)$		Differential acceptance $(K_L^0 \to l^+l^-/K_L^0 \to \pi^+\pi^-)$		Single event sensitivity
ee	2.99	ee	1.22	$Br(K_L^0 \to \mu e)$ 2.9×10^{-9}
μe	2.03	μe	0.69	$Br(K_L^0 \to ee)$ 2.0×10^{-9}
$\mu\mu$	1.27	$\mu\mu$	0.55	$Br(K_L^0 \to \mu\mu)$ 4.6×10^{-9}

Table 1: Summary of calculation of single event sensitivity for the rare two body decay modes.

5 Search for $K_L^0 \to \pi^0 l_1 l_2$

The data obtained were also used in a search for decays of the type $K_L^0 \to \pi^0 l_1 l_2$, where l_1 and l_2 are a muon or electron. This was motivated by the Yale-BNL group's proposal (BNL 845) to conduct a dedicated search for such modes, with a sensitivity on the order of 10^{-11} in branching ratio. The E780 detector was far from optimized for such a search however: the acceptance to these modes was quite small (less than 1% of the two body acceptance) and only covered a small range in dilepton invariant mass, from about 300 MeV/c^2 to the kinematic limit at 363 MeV/c^2; also poor time information on signals from the electromagnetic calorimeter ($\approx$ 100 ns.) made for potentially large backgrounds from the overlap of K_{l3} decays with uncorrelated neutrals. Discussions of the standard model phenomenology for the decay $K_L^0 \to \pi^0 ee$ can be found in other contributions to these proceedings, here I will only mention that the branching ratio for this is expected to be no larger than a few times 10^{-11}, and to be mostly CP violating, with $\frac{\epsilon'(\pi^0 ee)}{\epsilon}$ possibly of order unity in the K.M. model; a sufficiently sensitive measurement of this process could then provide a very interesting probe of CP violation, particularly if coupled with a measurement of the $K_S^0 \to \pi^0 ee$ branching ratio. Furthermore, since the standard model rate is highly suppressed, this process offers an interesting window to search for new physics. The prior experimental status is not very constraining[7]: $Br(K_L^0 \to \pi^0 ee) \leq 2 \times 10^{-6}$ and $Br(K_L^0 \to \pi^0 \mu\mu) \leq 2 \times 10^{-6}$. No limit exists for $Br(K_L^0 \to \pi^0 \mu e)$

In this search the decay $K_L^0 \to \pi^0\pi^+\pi^-$ plays much the same role as the decay $K_L^0 \to \pi^+\pi^-$ did in the two body search. Figures 5.1a,b,c show the reconstructed mass of π^0's from $K_L^0 \to \pi^0\pi^+\pi^-$ decay, as well the reconstructed kaon mass and θ^2 for those decays. In the latter set of plots, the energy of the two photons from the π^0 decay has been rescaled so as to obtain the correct value for the π^0 mass; the kaon mass resolution is 3.1 MeV/c^2, and a cut on $\theta^2 \leq 10^{-5} mr^2$ will be quite efficient to good events. For this sample, photon clusters were required to be isolated and such that 90% of the cluster energy was deposited in a 2×2 block area of the lead glass. Furthermore, clusters around the beam hole were ignored, and events with more than 2 clusters (other than those associated with the charged tracks) were rejected. For the rare modes, tighter particle identification requirements were applied than those used in the two body search. In particular, electrons were required to deposit at least 85% and no more than 140% of their energy in the lead glass; furthermore electron clusters (like photon clusters) were required to be such that at least 90% of the total cluster energy was deposited

in a 2×2 block area of the lead glass.

Furthermore, the charged particle invariant mass was used to calculate the dilepton momentum (P_{ll}) in the kaon rest frame, and the charged tracks were required to have a laboratory P_t no more than 5 MeV/c larger than P_{ll}, explicitly:

$$P_t \leq [(\frac{M_K^2+M_{\pi^0}^2-M_{ll}^2}{2M_K})^2 - M_{\pi^0}^2]^{1/2} + 5 \text{ MeV/c}.$$

Figures **5.2**a,b,c show mass vs θ^2 distributions for the rare decay modes. These distributions reflect the most up to date calibration of the electromagnetic calorimeter. No events consistent with signal are found in the $K^0 \to \pi^0\mu e$ sample (this allows us to set a 90% confidence limit on this decay mode of: $Br(K_L^0 \to \pi^0\mu e) \leq 4 \times 10^{-6}$, assuming a phase-space distribution); however there are one event each in the $K^0 \to \pi^0 ee$ and $K^0 \to \pi^0\mu\mu$ samples consistent with signal. Particulars of these events are shown in Table 2.

$K_L^0 \to \pi^0 e^+ e^-$				$K_L^0 \to \pi^0 \mu^+ \mu^-$			
$m(\gamma\gamma)$	$m(e^+e^-\gamma\gamma)$	θ^2 (mr^2)	$m(e^+e^-)$	$m(\gamma\gamma)$	$m(\mu^+\mu^-\gamma\gamma)$	θ^2 (mr^2)	$m(\mu^+\mu^-)$
140.5	487.5 481.3*	1.8	328.5	140.6	509.9 503.2*	3.8	332.8
$E(e^+)$	$E(e^-)$	$E(\gamma_1)$	$E(\gamma_2)$	$E(\mu^+)$	$E(\mu^-)$	$E(\gamma_1)$	$E(\gamma_2)$
7.4	5.6	2.1	1.3	2.9	2.6	2.4	1.8

Table 2: kinematic quantities for the candidate events. Mass is in units of MeV/c^2, energy in GeV.
* Mass calculated by setting the $\gamma\gamma$ mass to the π^0 mass.

The reconstructed kaon mass for the $K^0 \to \pi^0 ee$ candidate is quite low, 481 MeV/c^2, (it had been considerably higher!) so that the event loses much of its allure. Unfortunately however, for this decay mode radiative corrections lead to a significantly distorted reconstructed mass spectrum, when the radiated photons are missed, thus even though the candidate is a weak one it cannot be excluded; we calculate the probability for a genuine event of this type to reconstruct to a mass equal to or lower than 481 MeV/c^2 to be on the order of 17%.

The candidate has another potentially serious problem: there are extra hits in the A and B chambers which, although they do not define lines intersecting the decay vertex, could be interpreted as low energy tracks (a few hundred MeV or so) originating from the decay vertex, but distorted by the fringe field of the spectrometer magnet between the A and B chambers (about 6 MeV/c) and then swept out of the acceptance before reaching the C chamber. This is precisely the kind of thing one would expect from the following decay chain: $K^0 \to \pi^0\pi^0$ followed by the dalitz decay of each π^0. A subset of those instances were both π^0 dalitz decays are quite asymmetric, so that one of the electrons takes very little energy in the kaon rest frame, can give rise to precisely the sort of event which we observed. However, the *a priori* probability for this to occur in our data sample was estimated (using Monte Carlo methods) to be less than 0.5%.

Finally we estimated the background due to K_{e3} overlap with uncorrelated clusters in the lead glass to be on the order of 10% for the $K^0 \to \pi^0 ee$ decay mode. This was based on a study of such events, from the data itself. Although the procedure should be quite reliable, it is subject to a large

statistical error due to the paucity of these events, and the estimate given above could easily be off by a factor of two in either direction.

Similarly we estimated the background for the $K^0 \rightarrow \pi^0\mu\mu$ mode, from both event overlap and misidentified $K_L^0 \rightarrow \pi^0\pi^+\pi^-$ to be on the order of 20%, again with a large statistical uncertainty. However, for the $K_L^0 \rightarrow \pi^0\mu\mu$ candidate, a caviat is given by the fact that the two muon tracks overlap in the range stack, thus diminishing the μ/π discrimination.

Estimates of our sensitivity are such that, if the candidate events were indeed $K_L^0 \rightarrow \pi^0 l^+ l^-$ decays, they would imply branching ratios (assuming a phase-space distribution) of 1.1×10^{-6} and 4×10^{-6} for $K^0 \rightarrow \pi^0 ee$ and $K^0 \rightarrow \pi^0\mu\mu$ respectively. For the process $K_L^0 \rightarrow \pi^0 + X$, with $M_X = 330\ \mathrm{MeV/c^2}$, we calculate branching ratios of 2×10^{-7} and 8×10^{-7} for the two modes respectively.

Clearly these data are quite insufficient to constitute evidence for anomalously large branching ratios for the above processes, however they raise tantalizing possibilities. With this in mind several, relatively minor changes were made to the detector in order to maximize both the acceptance and bakground rejection for these decays, without however hindering the primary goal of this experiment. In particular, we implemented a feature on our ADC boards, which allows us timing of 10 ns for the rising edge of signals from the electromagnetic calorimeter. This should result in at least a factor 10 improvement in background rejection.

On February first, we started a new data taking period which is anticipated to end in mid-May.

A *preliminary* analysis of our status as of April 1, enables us to place an upper limit (at the 90% confidence level) $Br(K_L^0 \rightarrow ee) \leq 1.6 \times 10^{-9}$ (including the 1987 data); it also suggests that, with a single event sensitivity of approximately 2×10^{-7}, assuming a phase space distribution, no new events of the type $K_L^0 \rightarrow \pi^0 ee$ are contained in our data. That data set has yet to be analyzed for decay modes containing muons.

We anticipate a final single event sensitivity, by the end of this data taking period, of approximately 5×10^{-10} for the two body decay modes under study, and of approximately 10^{-7} for the three body decay modes.

References

(1) Kobayashi and Maskawa, Prog. Theor. Phys. **49** (1973)

(2) E. Farhi and L. Susskind, Phys. Rep. **74** (1981)

(3) R.N. Cahn and H. Harari, Nuc. Phys. **B176**, 135 (1980)

(4) L.J. Hall and L.J. Randall, Nuc. Phys. **B274**, 157 (1986)

(5) J.C. Pati, Phys. Lett. B **144**, 375 (1984)
J.C. Pati and H. Stremnitzer, Phys. Lett. B **172**, 441 (1986)

(6) B.A. Campbell, Phys.Rev. D VOL.28 N^{0}1, 209 (1983)

(7) M. Aguilar-Benitez *et al.* (Particle Data Group), Phys. Lett. **170B** (1986)

(8) W.C. Carithers *et al.* Phys. Rev. Lett. **30**, 1336 (1973) W.C. Carithers *et al.* Phys. Rev. Lett. **31**, 1025 (1973)

(9) Greenlee *et al.* Phys. Rev. Lett. **60**, 893 (1988)

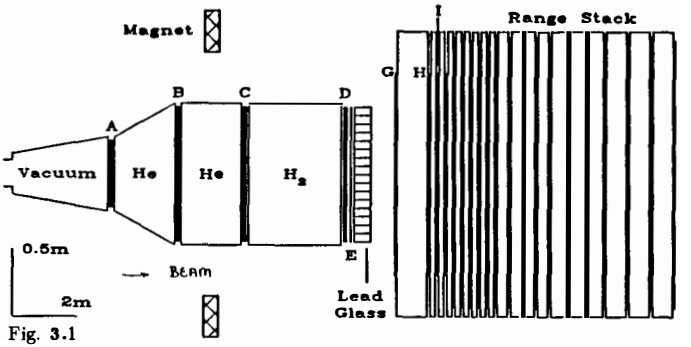

Fig. 3.1

3.1 : Plan view of the E780 detector

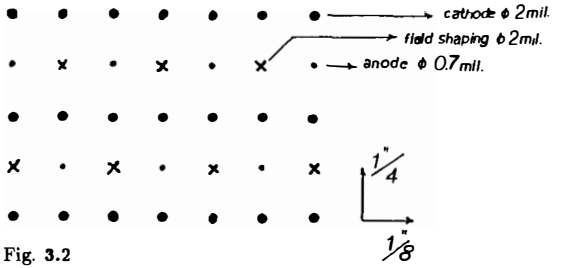

Fig. 3.2

3.2 : Mini-drift chambers cell structure

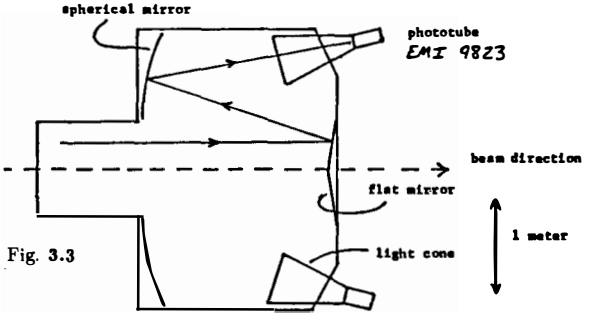

Fig. 3.3

3.3 : Schematic of Cerenkov counter, side view

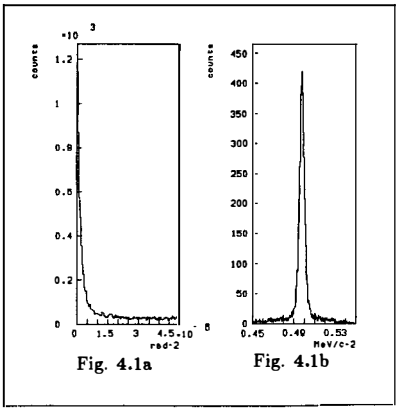

Fig. 4.1a Fig. 4.1b

4.1a : θ^2 for $K^0 \to \pi^+\pi^-$

4.1b : Reconstructed mass for $K^0 \to \pi^+\pi^-$

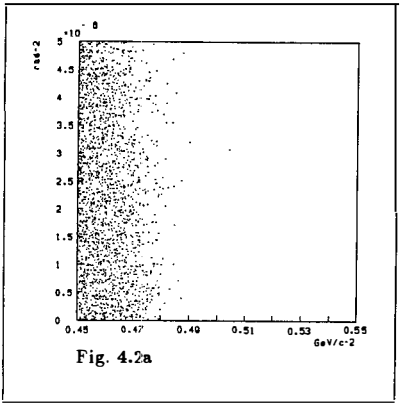

Fig. 4.2a

4.2a : Mass vs. θ^2 for $K^0 \to \mu e$

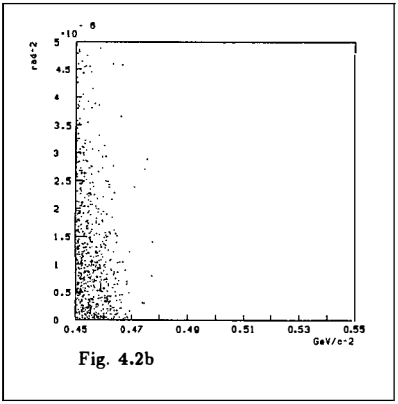

Fig. 4.2b

4.2b : Mass vs. θ^2 for $K^0 \to ee$

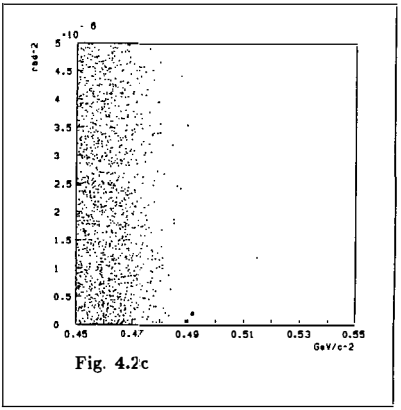

Fig. 4.2c

4.2c : Mass vs. θ^2 for $K^0 \to \mu\mu$

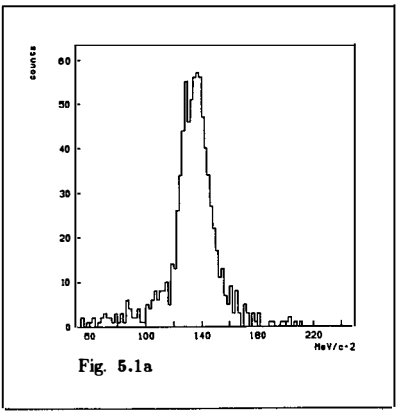

Fig. 5.1a

5.1a : Reconstructed π^0 mass, from $K_L^0 \to \pi^0\pi^+\pi^-$

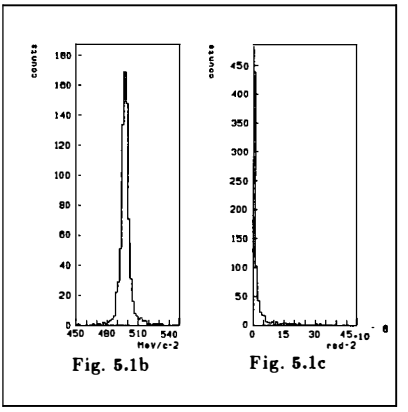

Fig. 5.1b

Fig. 5.1c

5.1b : Reconstructed kaon mass, for $K_L^0 \to \pi^0\pi^+\pi^-$

5.1c : θ^2 for $K_L^0 \to \pi^0\pi^+\pi^-$

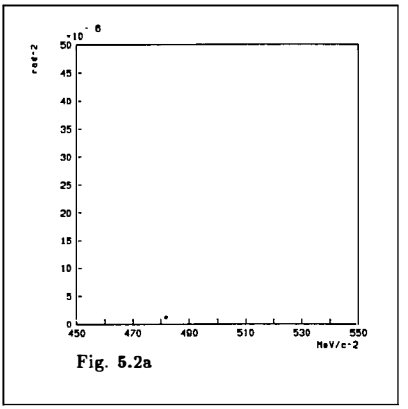

Fig. 5.2a

5.2a : Mass vs. θ^2 for $K_L^0 \to \pi^0 ee$

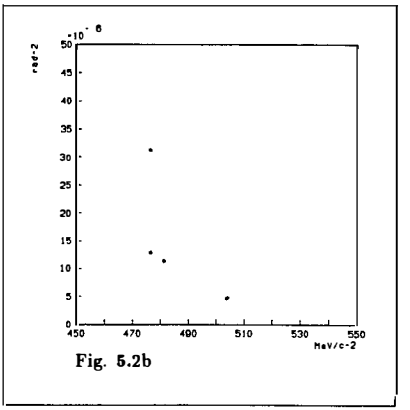

Fig. 5.2b

5.2b : Mass vs. θ^2 for $K_L^0 \to \pi^0 \mu\mu$

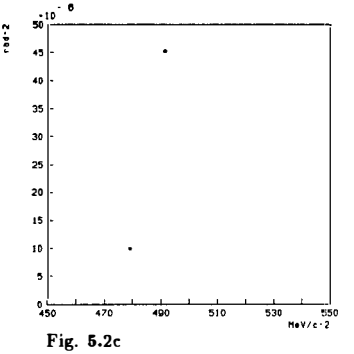

Fig. 5.2c

5.2c : Mass vs. θ^2 for $K_L^0 \rightarrow \pi^0 \mu e$